Research Article | Vol. 24, No. 21 | 17 Oct 2016 | OPTICS EXPRESS 24161

Optics EXPRESS

Design and fabrication of two-stack tandem-type all-phosphorescent white organic light-emitting diode for achieving high color rendering index and luminous efficacy

HYUNSU CHO,[1] CHUL WOONG JOO,[1] JONGHEE LEE,[1] HYUNKOO LEE,[1] JAEHYUN MOON,[1] JEONG-IK LEE,[1] JUN YEOB LEE,[2] YOUNGJIN KANG[3] AND NAM SUNG CHO[1,*]

[1] *Flexible Information Device Research Section, ICT Materials & Components Research Laboratory, Electronics and Telecommunications Research Institute (ETRI), 218 Gajeong-ro, Yuseong-gu, Daejeon, South Korea*
[2] *School of Chemical Engineering, Sungkyunkwan University, Suwon, 440-746, South Korea*
[3] *Division of Science Education, Kangwon National University, Chuncheon, 200-701, South Korea*
[*] *kevinchons@etri.re.kr*

Abstract: White organic light-emitting diodes (WOLEDs) are regarded as the general lighting source. Although color rendering index (CRI) and luminous efficacy are usually in trade-off relation, we will discuss about the optimization of both characteristics, particularly focusing on the spectrum of a blue emitter. The emission at a shorter wavelength is substantially important for achieving very high CRI (> 90). The luminous efficacy of a phosphorescent blue emitter is low as its color falls in the deeper blue range; however, that does not show any significant influence on the WOLEDs. WOLEDs with different blue dopants are compared to confirm the calculation of the CRI and luminous efficacy, and the optimized WOLEDs exhibit luminous efficacy of 38.3 lm/W and CRI of 90.9.

OCIS codes: (230.0230) Optical devices; (230.3670) Light-emitting diodes.

References and links

1. S. Jang, Y. Lee, and M. C. Park, "OLED lighting for general lighting applications," SID Symposium Digest of Technical Papers **46**(1), 661–663 (2015).
2. T. Komoda, N. Ide, K. Varutt, K. Yamae, H. Tsuji, and Y. Matsuhisa, "High-performance white OLEDs with high color-rendering index for next-generation solid-state lighting," J. Soc. Inf. Displ. **19**(11), 838–846 (2011).
3. K. Yamae, H. Tsuji, V. Kittichungchit, N. Ide, and T. Komoda, "Highly efficient white organic light-emitting diodes with over 100 lm/W for next-generation solid-state lighting," J. Soc. Inf. Displ. **21**(12), 529–540 (2014).
4. B. W. D'Andrade and S. R. Forrest, "White organic light-emitting devices for solid-state lighting," Adv. Mater. **16**(18), 1585–1595 (2004).
5. S. Reineke, M. Thomschke, B. Lüssem, and K. Leo, "White organic light-emitting diodes: Status and perspective," Rev. Mod. Phys. **85**(3), 1245–1293 (2013).
6. L. S. Liao, K. P. Klubek, and C. W. Tang, "High-efficiency tandem organic light-emitting diodes," Appl. Phys. Lett. **84**(2), 167–169 (2004).
7. T. Matsumoto, T. Nakada, J. Endo, K. Mori, N. Kawamura, A. Yokoi, and J. Kido, "Multiphoton organic EL device having charge generation Layer," SID Symposium Digest of Technical Papers **34**(1), 979–981 (2003).
8. J. Chen, F. Zhao, and D. Ma, "Hybrid white OLEDs with fluorophors and phosphors," Mater. Today **17**(4), 175–183 (2014).
9. J.-H. Jou, Y.-C. Chou, S.-M. Shen, M.-H. Wu, P.-S. Wu, C.-R. Lin, R.-Z. Wu, S.-H. Chen, M.-K. Wei, and C.-W. Wang, "High-efficiency, very-high color rendering white organic light-emitting diode with a high triplet interlayer," J. Mater. Chem. **21**(46), 18523–18526 (2011).
10. J.-H. Jou, S.-M. Shen, C.-R. Lin, Y.-S. Wang, Y.-C. Chou, S.-Z. Chen, and Y.-C. Jou, "Efficient very-high color rendering index organic light-emitting diode," Org. Electron. **12**(5), 865–868 (2011).
11. T. Zhang, S.-J. He, D.-K. Wang, N. Jiang, and Z.-H. Lu, "A multi-zoned white organic light-emitting diode with high CRI and low color temperature," Sci. Rep. **6**, 20517 (2016).
12. J. Lee, W. J. Sung, C. W. Joo, H. Cho, N. S. Cho, G.-W. Lee, D.-H. Hwang, and J.-I. Lee, "Simplified bilayer white phosphorescent organic light-emitting diodes," ETRI J. **38**(2), 260–264 (2016).

#273112 http://dx.doi.org/10.1364/OE.24.024161
Journal © 2016 Received 5 Aug 2016; revised 13 Sep 2016; accepted 30 Sep 2016; published 10 Oct 2016

Optics EXPRESS

13. C. W. Joo, J. Moon, J.-H. Han, J. W. Huh, J.-W. Shin, D.-H. Cho, J. Lee, N. S. Cho, and J.-I. Lee, "White transparent organic light-emitting diodes with high top and bottom color rendering indices," J. Inf. Displ. **16**(3), 161–168 (2015).
14. J. Lee, H.-F. Chen, T. Batagoda, C. Coburn, P. I. Djurovich, M. E. Thompson, and S. R. Forrest, "Deep blue phosphorescent organic light-emitting diodes with very high brightness and efficiency," Nat. Mater. **15**(1), 92–98 (2015).
15. H. Cho, J. Lee, J.-I. Lee, N. S. Cho, J. H. Park, J. Y. Lee, and Y. Kang, "Phenylimidazole-based homoleptic iridium(III) compounds for blue phosphorescent organic light-emitting diodes with high efficiency and long lifetime," Org. Electron. **34**, 91–96 (2016).
16. S. Chhajed, Y. Xi, Y.-L. Li, Th. Gessmann, and E. F. Schubert, "Influence of junction temperature on chromaticity and color-rendering properties of trichromatic white-light sources based on light-emitting diodes," J. Appl. Phys. **97**(5), 054506 (2005).
17. Q. Wang, J. Ding, D. Ma, Y. Cheng, L. Wang, and F. Wang, "Manipulating charges and excitons within a single-host system to accomplish efficiency/CRI/color-stability trade-off for high-performance OWLEDs," Adv. Mater. **21**(23), 2397–2401 (2009).
18. P. Vandersteegen, G. Schwartz, P. Bienstman, and R. Baets, "Luminous power efficiency optimization of a white organic light-emitting diode by tuning its spectrum and its extraction efficiency," Appl. Opt. **47**(11), 1947–1955 (2008).
19. J. Schwiegerling, Field Guide to Visual and Ophthalmic Optics (SPIE Press, 2004).
20. H. Cho, C. Yun, and S. Yoo, "Multilayer transparent electrode for organic light-emitting diodes: tuning its optical characteristics," Opt. Express **18**(4), 3404–3414 (2010).
21. J. Tae Lim, H. Lee, H. Cho, B.-H. Kwon, N. Sung Cho, B. Kuk Lee, J. Park, J. Kim, J.-H. Han, J.-H. Yang, B.-G. Yu, C.-S. Hwang, S. Chu Lim, and J.-I. Lee, "Flexion bonding transfer of multilayered graphene as a top electrode in transparent organic light-emitting diodes," Sci. Rep. **5**, 17748 (2015).
22. Y. Kawamura, S. Yanagida, and S. R. Forrest, "Energy transfer in polymer electrophosphorescent light emitting devices with single and multiple doped luminescent layers," J. Appl. Phys. **92**(1), 87–93 (2002).
23. S. H. Kim, J. Jang, and J. Y. Lee, "Improved efficiency in red phosphorescent organic light-emitting devices using double doping structure," Synth. Met. **157**(4–5), 228–230 (2007).
24. H. Sasabe, H. Nakanishi, Y. Watanabe, S. Yano, M. Hirasawa, Y.-J. Pu, and J. Kido, "Extremerly low operating voltage green phosphorescent organic light-emitting diodes," Adv. Mater. **23**, 5550–5555 (2013).
25. X. Ban, K. Sun, Y. Sun, B. Huang, S. Ye, M. Yang, and W. Jiang, "High power efficiency solution-processed blue phosphorescent organic light-emitting diodes using exciplex-type host with a turn-on voltage approaching the theoretical limit," ACS Appl. Mater. Interfaces **7**(45), 25129–25138 (2015).

1. Introduction

General lighting has been closely involved with our lives. Through the era of incandescent light bulbs and fluorescent lamps, inorganic light-emitting diodes (LEDs) have been a major light source for general lighting these days. Despite several advantages of LEDs in terms of efficiency and cost, organic light-emitting diodes (OLEDs) have attracted considerable attention [1–3]. Recently, the market of OLED lighting extended to not only general lighting but also specific lighting applications such as automobile lighting. This growth has stemmed from the unique properties of the OLEDs such as self-emissive area lighting source, thin and flexible form factor, and excellent color quality. Area lighting offers a uniform and smooth light, which provides its users with more comfortability. The flexibility of area lighting using OLEDs can unlock the potential from a design perspective against previous rigid lighting. The emission spectra of the OLEDs are close to those of sunlight, and their color temperatures are tunable over a wide range, opening possibilities of creating emotional comfort and physiological soothing effect. In addition, OLEDs are considered to be human-friendly lighting as they are completely free of UV light and involve lesser blue light risk than the LEDs. Despite these advantages, operational lifetime and luminous efficacy are the weak points of OLEDs as compared with LED light sources. In addition, the blue organic emitter was the main obstacle in the realization of commercial OLED products. Several organic stack structures have been suggested to generate white light: vertically stacked OLEDs, pixelated monochrome OLEDs, single-emitter-based WOLEDs, blue OLEDs with down-conversion layers, multiple-doped emission layers (EML), and single OLEDs with a sublayer EML [4–13]. Among various device architectures for fabricating WOLEDs, vertically stacked tandem structure has been regarded as the best solution because of its excellent luminous efficacy and operational stability [6–8]. In a tandem structure, emitting layers are not positioned adjacently but separated by charge generation layers, thereby providing electrically stable operations.

Optics EXPRESS

Among the organic emitters, phosphorescent green and red emitters have been demonstrated to impart sufficient efficiency and color. In contrast, color coordinate of phosphorescent blue emission is not deep enough. Therefore, the hybrid structures consisting of both phosphorescent red/ green emitters and fluorescent blue emitters are suitable for generating white light in commercial OLED products [8]. From the perspective of energy transfer, phosphorescent blue emitters offer inherently higher efficiency than fluorescent blue emitters. Thus, in order to achieve high efficiency and wide color realization in the WOLEDs, studies must be conducted on the efficiency and color of the phosphorescent blue emitters [14, 15].

In this paper, we discuss the relation between the CRI and luminous efficacy in tandem WOLEDs. In particular, we focus on the role of a blue dopant for CRI and efficiency. Among various characteristics of lighting, CRI and luminous efficacy serve as the pivotal parameters in evaluating the lighting quality. Light sources with high CRI (> 80) can reveal the accurate color of objects. Very high CRI (> 90) lightings are not only required for general lightings but also for special lighting environments such as surgery, museums, and photography venues [9–11]. In WOLEDs with tandem structures, it is difficult to realize a superior device that satisfies high efficiency and high CRI simultaneously because there is generally a trade-off between them [16–18]. Instead, the literatures reveal that these may be optimized in a single device.

2. WOLED simulation

2.1 Optimization of CRI

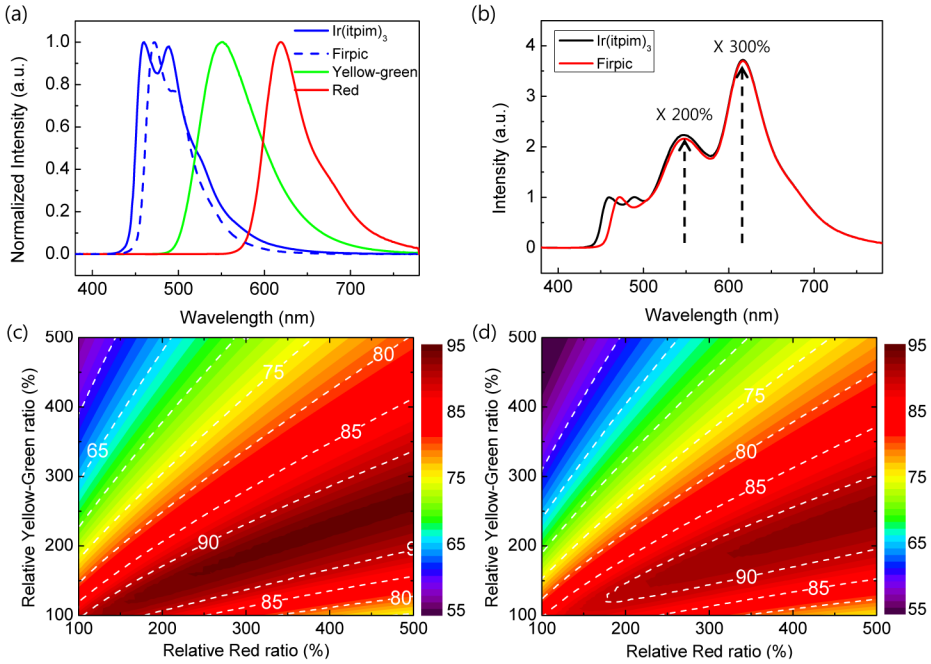

Fig. 1. (a) Electroluminescence (EL) spectra of FIrpic and $Ir(itpim)_3$. The EL spectra of red and yellow-green are also plotted. (b) The example of arbitrary white spectrum constructed by the relative portion of blue: yellow-green: red spectrum = 1:2:3. CRI of arbitrary white spectra with (c) Ir(itpim)3 and (d) FIrpic dopant according to the portion of red (x-axis) and yellow-green (y-axis).

In this study, two phosphorescent blue dopants were employed: bis[2-(4,6-difluorophenyl)pyridinato-N,$C^{2'}$](picolinato)iridium(III) (FIrpic) and a new material tris[2-(4-fluorophenyl)-1-(5′-isopropyl-(1,1’:3′,1”-terphenyl)-2’-yl)-1H-imidazole] iridium(III) ($Ir(itpim)_3$) [15]. The external quantum efficiency (EQE) of $Ir(itpim)_3$ with the host material

Optics EXPRESS

3,3-di(9H-carbazol-9-yl)biphenyl (mCBP) is higher than 20%. This value is comparable to that of FIrpic. As it can be seen in Fig. 1(a), the emission of $Ir(itpim)_3$ is in a deeper blue range than that of FIrpic. The first emission peaks of $Ir(itpim)_3$ and FIrpic are located at wavelengths 460 nm and 472 nm, respectively. The emission spectra of yellow-green and red, also plotted in Fig. 1(a), were used as the basis to obtain white spectra. Various white spectra can be constructed by varying the portions of yellow-green (y_G) and red (x_R) emission as follow:

$$S_W = x_R S_R + y_G S_G + S_B, \tag{1}$$

where S_W, S_R, S_G, and S_B are the emission spectra of white, red, yellow-green, and blue, respectively. For example, with a ratio of yellow-green to red as x_R:y_G = 2:3, one obtains an S_W as shown in Fig. 1(b). Because the first peak of $Ir(itpim)_3$ is at a shorter wavelength than that of FIrpic, S_W using $Ir(itpim)_3$ spans a wider wavelength region.

Figures 1(c) and (d) are the CRI contour plots of arbitrary S_W with $Ir(itpim)_3$ and FIrpic, and various relative ratios of red and yellow-green. Wide-ranging CRI values can be obtained by varying the relative augmentation ratio of yellow-green and red. Both the figures share common features. A high CRI is obtained at high portion of x_R and low portion of yellow-green y_G. Both blue dopants can achieve very high CRI (> 90) if red and yellow-green portions are well controlled. However, $Ir(itpim)_3$ offers a wider latitude in achieving high CRI than FIrpic. Comparing the Figs. 1(c) and 1(d), the area where the CRI of S_W is over 90 is broader for S_W with $Ir(itpim)_3$ than that with FIrpic, and its portion is 21.7% and 13.7%, respectively. In addition, for a given pair of x_R and y_G, $Ir(itpim)_3$ yields a larger CRI than FIrpic. For instance, with x_R = 350% and y_G = 200% in Eq. (1), the CRI values of S_W using $Ir(itpim)_3$ and FIrpic are 94.3 and 92.2, respectively. The highest attainable CRI with $Ir(itpim)_3$ is 94.4 at x_R = 380% and y_G = 220%. On the other hand, the highest CRI with FIrpic is 92.6, obtained at x_R = 500% and y_G = 250%. The results of Figs. 1(c) and 1(d) strongly indicate the importance of the presence of emission at shorter wavelengths in achieving high CRI WOLEDs.

2.2 Optimization of luminous efficacy

It is possible to obtain identical CRI with various combinations of red and yellow-green ratios. In order to suggest a guideline for obtaining high CRI and luminous efficacy simultaneously, it is useful to establish a relation between them. The luminous efficacy (η_P) can be calculated from the luminous flux (F) and electrical power (P) as [16–18]:

$$\eta_P = \frac{F}{P} = \frac{683.0\int E_{El}(\lambda)\eta_{oc}V(\lambda)d\lambda}{\int E_{El}(\lambda)\frac{1}{\eta_{\text{int}}}\frac{qV\lambda}{hc}d\lambda}, \tag{2}$$

where $E_{El}(\lambda)$ and η_{oc} are the normalized radiant flux and outcoupling efficiency of OLED devices; η_{int} is the internal quantum efficiency, i.e., the amount of excitons needed to create one photon; $V(\lambda)$ is the photopic response curve [19]; h is the Planck constant; c is the light speed; V is the operating voltage; λ is the wavelength; and $hc/qV\lambda$ represents the relation between the optical power of the photon and energy for creating the exciton. In conjunction with Eq. (2), we have used the spectral data of Figs. 1(c) and 1(d) to obtain the η_p. This allows us to establish the mutual relation between the CRI and luminous efficacy. Figures 2(a) and 2(b) show the luminous efficacy of arbitrary white spectrum S_W with $Ir(itpim)_3$ and FIrpic. For two-stacked tandem OLEDs, we have used 40% for η_{oc}, 100% for η_{int}, and 7 V for V, respectively, and these values are based on our experimental results discussed in the section 3.

Optics EXPRESS

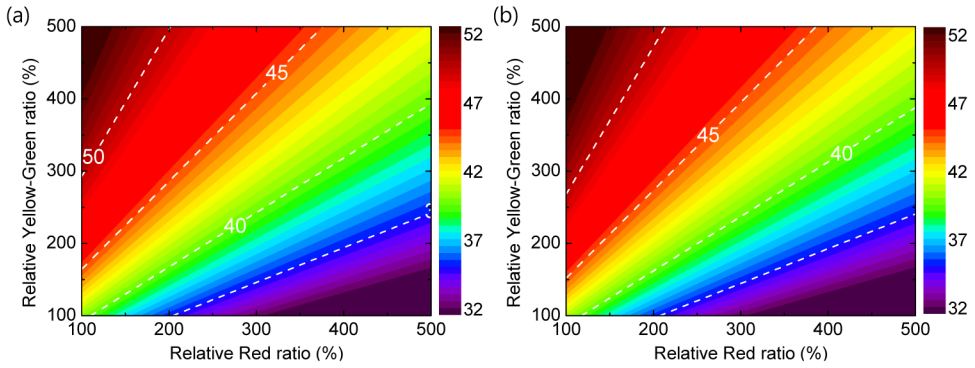

Fig. 2. Luminous efficacy of arbitrary white spectra with (a) $Ir(itpim)_3$ and (b) FIrpic dopant according to the red (x-axis) and yellow-green (y-axis) portions.

As shown in Figs. 2(a) and 2(b), emission ratios of yellow-green dominantly influence the luminous efficacy. As the portion of yellow-green emission increases, the luminous efficacy of the WOLEDs increases proportionally; however, the CRI decreases, as shown in Figs. 1(c) and 1(d). Our calculation results of Fig. 2 are in accordance with the general trade-off relationship between the CRI and luminous efficacy in the WOLEDs. On the other hand, blue emission has a limited impact on the luminous efficacy in the WOLEDs. Unlike the results of Figs. 1(c) and 1(d), the calculated luminous efficacies of two blue dopants are more or less similar. In particular, the portion of blue emission is quite limited and their impact on the luminous efficacy is marginal at CRI higher than 90. For instance, with x_R = 350% and y_G = 200%, the CRI values of the WOLEDs using $Ir(itpim)_3$ and FIrpic are 94.3 and 92.2, respectively. However, the luminous efficacies are almost identical at 36.4 lm/W and 36.5 lm/W. Because the photopic response of blue is fairly low [19], high EL emission at a short wavelength does not necessarily yield a high luminous efficacy.

2.3 Optimization of a device structure

In this section, we aim to elaborate our two-stack tandem structure by locating the positions of the emission layers and determining the thicknesses of common organic layers. First, to achieve a high CRI, the location of red, yellow-green, and blue emitters is determined. Because three colors were used in the two-stack tandem structure, at least two colors must be located in a single stack. Referring to Figs. 1 (c) and 1(d), a high CRI is obtained with a high red fraction. For example, WOLEDs with a CRI of 93.6 are obtained at a ratio of red: yellow-green: blue = 3:2:1. Thus, to achieve a strong emission from red, it is preferred to insert red in a single stack and the others in another stack.

In the next step, the thicknesses of common organic layers were determined to optimize the optical effect. Figures 3(a) and 3(b) show the EQE contour plots of blue and red emissions as functions of hole transporting layer (HTL) and electron transporting layer (ETL) thicknesses using an optical simulation program (Setfos, Fluxim). The simulation parameters, including the thicknesses of the HTL and ETL, range from 50 nm to 350 nm in a device structure made of Glass/ indium tin oxide (ITO) (70 nm)/ HTL (x nm)/ EML (10 nm)/ ETL (y nm)/ Al (100 nm). The spectral characteristics of blue (FIrpic) and red were obtained from Fig. 1(a). For a given ETL or HTL thickness, the change in the EQE for each emission is almost complementary. At x = 200 nm and y = 170 nm, the simulated EQE of blue is the highest, while the EQE of its counterpart is the lowest. Using the simulation results of Fig. 3, it is possible to deduce the ETL and HTL thickness pairs, which correspond to resonance conditions. Because the ETL thickness determines the distance between the emissive layer and reflective cathode, the effect of ETL thickness is more significant than the HTL thickness [20].

Optics EXPRESS

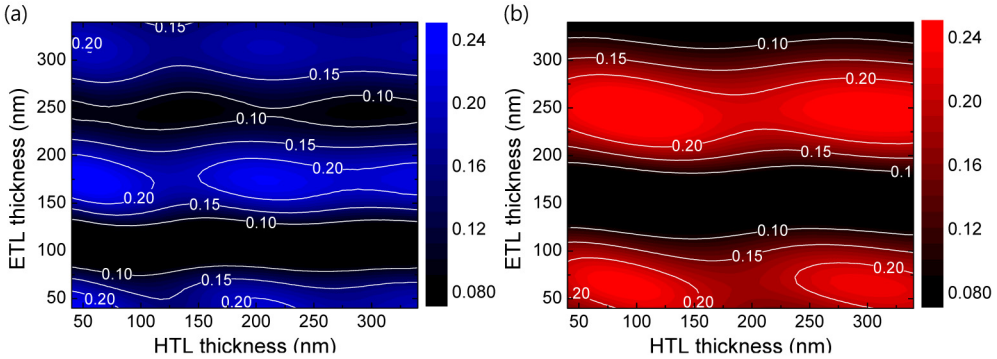

Fig. 3. External quantum efficiency (EQE) contour plots of (a) blue and (b) red emissions as functions of the hole transporting layer (HTL) and electron transporting layer (ETL) thicknesses.

Table 1. Two-stack tandem structure designs based micro-cavity approach

	EML-1: Red, EML-2: Blue			EML-1: Blue, EML-2: Red		
	Blue	Red	Final thickness	Red	Blue	Final thickness
ETL-2	50 nm		50 nm	70 nm		70 nm
EML-2	10 nm		10 nm	10 nm		10 nm
HTL-2 Charge generation layer (CGL) ETL-1	360 nm (3rd cavity)	250 nm (2nd cavity)	190 nm	300 nm (2nd cavity)	180 nm (2nd cavity)	100 nm
EML-1		10 nm	10 nm		10 nm	10 nm
HTL-1		90 nm (1st cavity) 290 nm (2nd cavity)	disparity		200 nm (2nd cavity) 360 nm (3rd cavity)	~190 nm

Generally, two-stack tandem OLEDs consist of ITO, two HTLs, two ETLs, two EMLs, a CGL, and a cathode. The stack structure may be expressed as substrate/ ITO/ HTL-1/ EML-1/ ETL-1/ CGL/ HTL-2/ EML-2/ ETL-2/ Al. A red or blue emission layer could be placed in the proximity of the substrate. The thicknesses of the emissive layers, EML-1 and EML-2, were fixed as 10 nm each, which is a commonly used thickness in real device fabrication. We start with the case of blue as the EML-2. First, based on Fig. 3(a), the first resonance thickness of ETL-2 was determined as 50 nm. Next, based on Fig. 3(b), the second resonance thickness of the ETL for red was determined as 250 nm. Because the thickness of EML-2 was fixed as 10 nm, the combined thickness of HTL-2, CGL, and ETL-1 was 190 nm. Therefore, the thickness of the HTL for blue should be larger than 190 nm. The third resonance thickness of the HTL for blue was determined to be 360 nm. Finally, this gives the thickness of HTL-1 as 160 nm. However, referring to Fig. 3(b), a thickness of 160 nm does not correspond exactly to the resonance thickness of HTL-1 for red. (The first and second resonance thicknesses of the HTL for red are 90 nm and 290 nm, respectively.) Thus, due to the disparity in resonance conditions of blue and red emission, the thicknesses of organic part corresponding to HTL-1 have to be compromised on the basis of Fig. 3.

An approach identical to EML-2 can be applied to the other case of red. A red emission layer is close to the Al cathode; therefore, the thickness of ETL-2 thickness selected as 70 nm is regarded as the first cavity length for red. Using the same principal as stated above, the total thickness of HTL-2, CGL, and ETL-1 is selected as 100 nm to optimize the blue emission. Unlike the previous result, the thickness of HTL-1 satisfies both the second cavity length for the blue and red emissions. Therefore, it is rational to have red and blue in the

Optics EXPRESS

proximity of the Al cathode and substrate, respectively. Two suggested stack structures are presented in Table 1.

3. Experiments & results

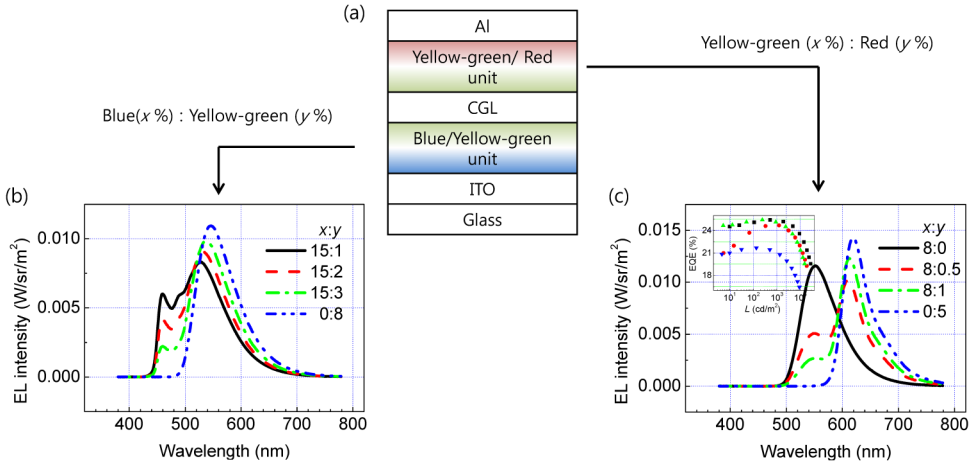

Fig. 4. (a) Device structure of tandem WOLED and the EL spectra of (b) 1st and (c) 2nd EML as a function of relative doping concentration. Inset: the EQE of 2nd EML-based unit device as a function of relative doping concentration.

To fabricate WOLEDs with high CRI and high efficiency, the CRI and efficiency simulation results were adopted as our guideline. The bluish emitting layer was positioned in the proximity of the substrate and the reddish emitting layer in the proximity of the metallic cathode. The actual stack structure of our WOLED device is Glass/ ITO (70 nm)/ HTL (190 nm)/blue: yellow-green EML (10 nm)/ ETL (20 nm)/ CGL (50 nm)/ HTL (45 nm)/ yellow-green: red EML (10 nm)/ ETL (70 nm)/ LiF/ Al, whose cross-sectional schematics are shown in Fig. 4(a). The information about used materials for blue: yellow-green unit [15] and yellow-green: red unit were provided in previous works [21]. In addition, CGL consisted of Li-doped ETL [21] and 1,4,5,8,9,11-hexaazatriphenylenehexa carbonitrile (HAT-CN). The thickness of each organic component is based on the results of section 2.3. To achieve a high CRI, the relative concentrations of the emitting dopants in the first and second emitting layers were carefully adjusted as discussed in section 2.1. Figures 4(b) and 4(c) show the EL intensity of each unit for different doping ratios. As the concentration of the low-energy dopant increases, the energy transfer between two dopants increases, resulting in enhanced emission of the low-energy dopant [22]. Unlike the structure used in the simulation, the reddish EML in the actual device consisted of a mixture of yellow-green and red dopants instead of the red-only dopant. As shown in the inset of Fig. 4(c), the unit device including yellow-green dopants exhibited improved EQE of 15% than one with only red dopant. This is because a yellow-green dopant can induce efficient energy transfer from host material to red dopant and contribute to increase in the efficiency [23].

Figure 5(a) shows the current density (J)–voltage (V)–luminance (L) characteristics of the tandem WOLEDs. While the reddish EML is common, the blue dopants differ with respect to $Ir(itpim)_3$ and FIrpic. The measured J–V–L characteristics did not turn out to be strong functions of the dopant type. Both devices have a turn-on and operating voltages of 5.5 V and 7 V, respectively. The former and latter correspond to voltages required to achieve luminance levels of 1 cd/m^2 and 1,000 cd/m^2, respectively. Optimized single stack red and green OLEDs have a turn-on voltage of about 2.5 V [24]. Owing to the high energy requirement, the turn-on voltage of the blue OLEDs is approximately 3 V [25]. Considering the turn-on voltages of

Optics EXPRESS

these single stack OLEDs, our tandem OLEDs work almost ideally. We attribute the adequate extent of electrical characteristics to our CGL, which enables seamless electrical transport.

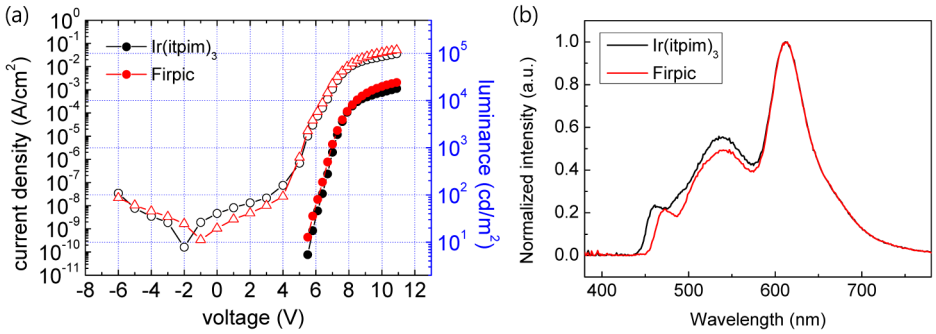

Fig. 5. (a) Current density (*J*)–voltage (*V*)–luminance (*L*) characteristics and (b) the normalized electroluminescence (EL) intensity of the WOLEDs.

Figure 5 (b) shows the normalized EL intensities of the WOLEDs measured by using an integrating sphere. Measured efficiencies and CRIs are summarized in Table 2. As discussed in Section 2.1, tandem WOLEDs with $Ir(itpim)_3$ exhibit higher CRI than those with FIrpic. The stronger emission in shorter wavelength makes it possible to achieve a CRI higher than 90. The device efficiency of tandem WOLEDs with $Ir(itpim)_3$ is slightly higher than that with FIrpic. This is because the blue unit itself has different efficiency for two dopants, although it is less affected by a blue emitter, as discussed in the Section 2.2. Moreover, unlike the arbitrary white spectra in simulation, by simply adding the spectra for each color, the actual emission spectrum of the WOLEDs can be influenced by the cavity effect. This can also cause a difference between the measured and calculated data.

Table 2. Efficiency and CRI of 2-stacked tandem WOLEDs at 2.5 mA/cm²

	EQE (%)	PE (lm/W)	CRI	Color coordinate
$Ir(itpim)_3$	39.86	38.34	90.94	(0.452, 0.439)
FIrpic	36.58	35.63	88.76	(0..475, 0.449)

4. Conclusion

As an effort to deduce guidelines for obtaining high luminous efficacy and high CRI simultaneously in WOLEDs, optical simulations on two-stack tandem OLEDs were conducted. The relative position of the EMLs in the tandem structure and the thickness of common organics can be determined based on the microcavity approach. Because the emissions from red and yellow-green are much stronger than that from blue, the overall luminous efficacies of the WOLEDs are not dominated by the blue emission. From the perspective of high CRI, it is, however, important to achieve a balanced emission. Our simulations show that not only strong red emission is desirable but also the presence of deep blue emission is crucial in obtaining high CRI. Both high luminous efficacy (38.3 lm/W) and CRI (90.9) were achieved by blue phosphorescent $Ir(itpim)_3$-based device. Our design approaches and experimental demonstration of two-stack tandem WOLEDs suggest a practical guide for preparing high-quality WOLED light sources.

Funding

Ministry of Trade, Industry, and Energy/Korea Evaluation Institute of Industrial Technology (MOTIE/KEIT) (10045269)